Journal of Alloys and Compounds 504 (2010) 535–541

Contents lists available at ScienceDirect

Journal of Alloys and Compounds

journal homepage: www.elsevier.com/locate/jallcom

Effect of electromigration on intermetallic compound formation in line-type Cu/Sn/Cu interconnect

L.D. Chen, M.L. Huang*, S.M. Zhou

Electronic Packaging Materials Laboratory, School of Materials Science & Engineering, Dalian University of Technology, No. 2 Linggong Road, Liaoning, Dalian 116024, China

ARTICLE INFO

Article history:
Received 28 February 2010
Received in revised form 19 May 2010
Accepted 29 May 2010
Available online 11 June 2010

Keywords:
Electromigration
Cu/Sn/Cu interconnect
Interfacial reaction
Intermetallic compound

ABSTRACT

The line-type Cu/Sn/Cu interconnects were used to determine the growth kinetics of interfacial intermetallic compounds (IMCs) under current densities ranging from 5.0×10^3 to 1.0×10^4 A/cm^2 at 100 and 150 °C, respectively. EM caused a polarity effect, i.e., the IMCs at the anode side were thicker than those at the cathode side. Compared with the aging specimens, the growth kinetics of the IMCs at the anode side during EM was significantly enhanced and still followed the $t^{1/2}$ law. The growth behavior of the IMCs at the cathode side was complicated. A growth model of the IMC at the cathode side was established. When the initial interfacial IMCs were very thin, J_{dis} was minute compared with $J_{em} + J_{chem}$. The inward fluxes were larger than the outward fluxes, and thus the IMCs grew. After the IMCs reached a critical thickness, J_{dis} became lager than $J_{em} + J_{chem}$. The inward fluxes were less than the outward fluxes, and thus the IMCs decreased in thickness.

1. Introduction

With the continuous increasing in the I/O number of chips, the flip chip solder joints are downsizing and the current density applied to the solder joints is up to 10^4 A/cm^2. Now electromigration (EM) becomes a serious reliability issue in high density packaging [1]. It is well known that EM is a mass transportation caused by the directional electron flow, which is also a diffusion phenomenon under a driving force. A significant current crowding occurs at the entrance of an actual flip chip solder joint, because the cross-section of the solder bump is two orders of magnitude larger than that of the Al interconnect wire [2]. Also due to the different electrical resistances and thermal capacities between the solder bump and the interconnect wire, it is possible that a considerable temperature gradient happens across the solder joint. This temperature gradient can cause additional thermomigration [3]. Actually, EM in a real flip chip solder joint is very complicated, which usually contains three effects: EM effect, current crowding effect and thermomigration effect.

The effect of EM on the solder joints has been studied [4–11]. Chen and co-workers [4] investigated the effect of moderate electric current density on mechanical properties of Ni–P/Sn–3.5Ag/Ni–P and Ni/Sn–3.5Ag/Ni solder joints and found that the EM caused brittle failure of the solder joints and this tendency for brittle failure increased with increasing current density. Ho and co-workers [5] investigated the EM effect on the Cu–Ni cross-interaction in Cu/Sn/Ni diffusion couples and found that the Cu–Ni cross-interaction strongly depended on the direction of electron flow. Chen and Huang [6] found that Ag_3Sn phase can intercept the Bi migration from the cathode side to the anode side after Ag was doped into Sn–58Bi solder. Chuang and co-workers [7] investigated the EM behavior of Sn–3Ag–0.5Cu and Sn–3Ag–0.5Cu–0.5Ce–0.2Zn solder joints at room temperature with a current density of 3.1×10^4 A/cm^2 and found that after dopping with Zn and Ce the EM process of Sn–Ag–Cu solder joints were accelerated due to the refinement of the solder matrix. Zhang and co-workers [8] found an abnormal polarity effect after direct current was applied to the Cu/Sn–9Zn/Cu interconnect, i.e., the IMC at the cathode side was thicker than that at the anode side, which was in contrast to the Cu/In/Cu and Cu/Sn–Pb/Cu interconnects [9,10]. Lin and co-workers [11] investigated the EM behavior of Cu/Sn–8Zn–3Bi/Cu interconnects and found that Bi is the dominant migrating species but Sn and Zn are relatively immobile under EM at 80 °C. The EM behavior is very complicated in solder interconnects, since different effects may be dominant when the current is applied to the different types of solder interconnects at different temperatures. In these EM studies, the initial interfacial IMCs in the interconnects were thick, while the initial IMC thickness may play an important role during EM which may affect the IMC growth behavior. In order to identify the effect of EM on the growth behavior of the interfacial IMCs, the immersing soldering was used to obtain a thin IMC layer in the present work.

At present, most lead-free solders are Sn-rich alloys, and the properties of Sn dominate the solders' behavior because of the high content of Sn (more than 95 wt.%). So it is important to under-

* Corresponding author. Tel.: +86 411 84706595; fax: +86 411 84709284.
E-mail address: huang@dlut.edu.cn (M.L. Huang).

0925-8388/$ – see front matter © 2010 Elsevier B.V. All rights reserved.
doi:10.1016/j.jallcom.2010.05.158

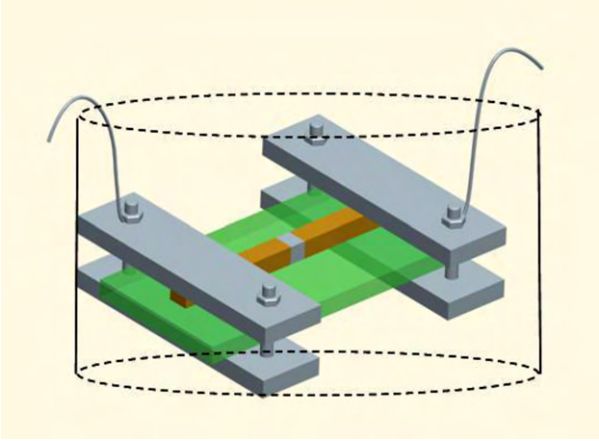

Fig. 1. Schematic of the experimental line-type Cu/Sn/Cu interconnect.

stand the interfacial reactions between pure Sn and the substrate metallizations, especially under high current density.

In this study, the line-type Cu/Sn/Cu interconnects were prepared in order to understand the fundamentals of the EM mechanism in high-Sn lead-free solder joints. The current crowding effect and thermomigration are expected to be avoided in this line-type interconnects because of their symmetric structure.

2. Experimental procedures

The line-type Cu/Sn/Cu interconnects were prepared by immersing soldering. Before soldering, two small copper plates (7 mm × 5 mm × 12 mm) were prepared. Of each plate, one face (5 mm × 7 mm) was carefully ground, polished, and cleaned in ethanol. Both of the polished faces were immediately electroplated with Sn film of 3 μm in thickness to improve the wettability and to avoid the void formation during soldering, and then the two Cu plates were aligned and fixed. After that the assembly was immersed into Sn bath at 260 °C for 10 s. The space between the two Cu plates was controlled by the spacers (two stainless steel lines of 500 μm in diameter). After soldering the interconnects were cooled in water to room temperature and then cut into slender bars with a cross-section of 600 μm × 600 μm by electric discharge machining. Finally, the cross-section of line-type interconnects were ground and polished down to 300 μm × 300 μm.

The EM experiments were conducted in silicone oil with a direct current applied to the line-type interconnects. Fig. 1 shows the schematic of the experimental configuration. The temperatures of the solder interconnects were 100 ± 4 and 150 ± 4 °C, respectively, which were monitored by a K-type thermocouple placed close to them. The applied current densities ranged from 5.0×10^3 to 1.0×10^4 A/cm^2. The EM durations ranged from 0 to 200 h. In order to compare with the EM effect, the reference Cu/Sn/Cu specimens were aged at the same temperatures for the same durations. After EM and aging, the specimens were taken out from the silicone oil and cooled in air to room temperature.

The microstructural evolution of the line-type interconnects during EM and aging was examined using scanning electron microscopy (SEM). An energy dispersive X-ray spectrometer (EDX) was used to identify the chemical compositions of the precipitates and phases between Sn and the substrate. The areas of the IMC layers were measured with an imaging processing software, and the thicknesses of the IMC layers were determined by dividing the area with linear length of the interface. So the thickness of the IMC layers was an average value measured from the selected area.

3. Results and discussion

3.1. Interfacial IMC growth of aging specimens (no-current case)

Fig. 2 shows the cross-section microstructure of the as-soldered line-type Cu/Sn/Cu interconnect after polishing. It is clear that Sn and Cu were well metallurgy soldered and no microvoids were observed in the as-soldered specimen. The as-soldered Sn/Cu interface is shown in Fig. 3(a). The initial interfacial Cu_6Sn_5 IMC layer in the as-soldered state was 0.37 μm in thickness, and a thin Cu_3Sn layer was expected to be formed between Cu_6Sn_5 and Cu, though it was difficult to be identified in SEM image. Fig. 3(b) and (c) shows the microstructure of the interfacial IMCs after being aged at 100 and 150 °C for 200 h, respectively. The thickness of the interfacial IMCs increased with the increasing aging time. It was 1.16 μm after being aged at 100 °C for 200 h, and 3.58 μm after being aged at 150 °C for 200 h. In addition, the interfacial IMCs gradually transformed from scallop-type to layer-type with the increasing aging time. Since there was no EM effect, the interfacial IMCs at both sides in the Cu/Sn/Cu interconnect were similar in thickness.

The diffusivity increased with the increasing temperature according to Arrhenius relationship, as expressed in Eq. (1). Thus the kinetics of the interfacial reaction at 150 °C was higher than that at 100 °C:

$$D = D_0 \exp\left(\frac{-Q}{RT}\right) \quad (1)$$

where D is the diffusivity, R is the gas constant, D_0 is a pre-exponential coefficient, Q is the activation energy, T is the absolute temperature.

The growth kinetics of the IMC layers at the Sn/Cu interface during aging was expressed by an empirical power-law relationship:

$$h_t - h_0 = Kt^n \quad (2)$$

where h_t is the average thickness of the IMC layers at time t, h_0 is the initial thickness ($t = 0$), K is the growth rate constant, and n is the time exponent. The value of n can be obtained by the multivariable linear regression analysis.

Fig. 4 shows the log plot of the growth kinetics of the interfacial IMCs during aging. The values of the time exponent n were 0.58 and 0.44 at 100 and 150 °C, respectively. It is considered that the diffusion process dominated the growth of the IMC layers, since the time exponents were similar to 0.5.

3.2. Interfacial IMC growth of EM specimens (applied with current)

Fig. 5 shows the interfacial IMCs at the anode side after being applied with the current densities of 5.0×10^3 and 1.0×10^4 A/cm^2 at 100 °C for various times. The SEM micrographs in the left column are for the current density of 5.0×10^3 A/cm^2 and those in the right column are for the current density of 1.0×10^4 A/cm^2. The IMCs at the anode side gradually changed from scallop-type to layer-type as the IMCs grew with the increasing time, and the IMCs at the anode side of the specimens after EM were flatter than that after being aged (no-current case). After EM under the current density of 5.0×10^3 A/cm^2 at 100 °C for 200 h, the average thickness of the IMCs at the anode increased to 1.97 μm, which was 1.70 times thicker than that of the no-current case at 100 °C for 200 h. After EM

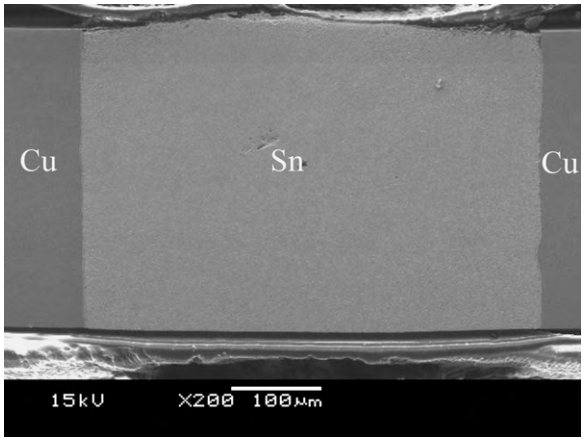

Fig. 2. Cross-section microstructure of the as-soldered line-type Cu/Sn/Cu interconnect.

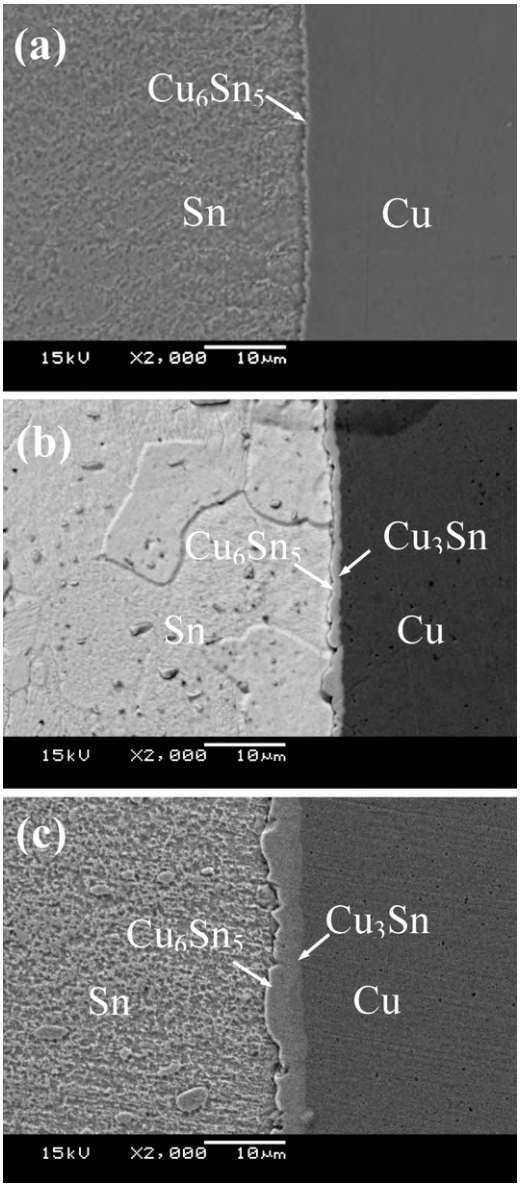

Fig. 3. SEM micrographs of the IMCs at the Sn/Cu interfaces during aging: (a) as-soldered, (b) after aging at 100 °C for 200 h, and (c) after aging at 150 °C for 200 h.

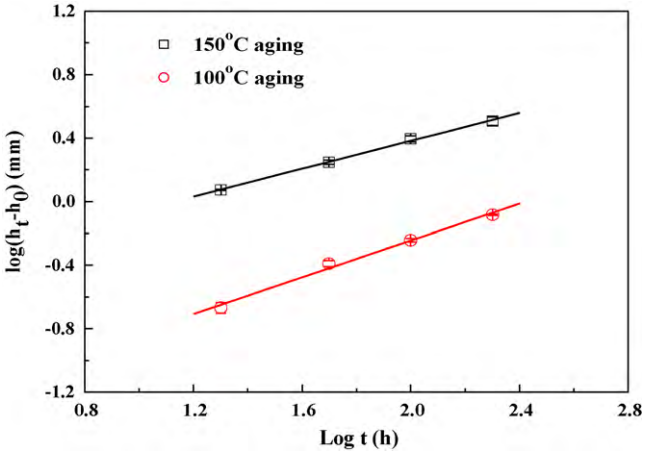

Fig. 4. Log plot of the growth kinetics of IMC layers at the Sn/Cu interface during aging.

under the current density of 1.0×10^4 A/cm^2 at 100 °C for 200 h, the average thickness of the IMCs at the anode side increased to 3.77 μm, which was 3.25 times thicker than that of the no-current case (being aged at 100 °C for 200 h). EM significantly enhanced the growth of the IMCs at the anode side in this study, which is in good agreement with the literature. Gan and Tu [12] also found that the EM enhanced the growth of the IMCs at the anode side under the current density of 1.0×10^4 A/cm^2 compared with that of the aging case. Furthermore, the interfacial IMCs in the right column were thicker than those in the left column, which demonstrated that the IMCs at the anode side grew faster under higher current density.

Fig. 6 shows the interfacial IMCs at the anode side after being applied with the current densities of 5.0×10^3 and 1.0×10^4 A/cm^2 at 150 °C for various times. Under the same current density, the growth kinetics of the IMCs at 150 °C was higher than those at 100 °C. After EM under the current density of 5.0×10^3 A/cm^2 at 150 °C for 200 h, the average thickness of the IMCs at the anode side increased to 7.84 μm, which was 2.19 times thicker than that of the no-current case (being aged at 150 °C for 200 h). After EM under the current density of 1.0×10^4 A/cm^2 at 150 °C for 200 h, the average thickness of the IMCs at the anode side increased to 12.15 μm, which was 3.39 times thicker than that of the no-current case. The effect of EM on the growth of the IMCs was more significant at higher temperature. Similarly, the IMCs at the anode side after EM at 150 °C were flatter than that of the no-current case at 150 °C.

The main difference between the aging specimens and EM specimens is the driving force for atom movement. The driving force in the aging specimens is chemical potential; while that in the EM specimens includes both chemical potential and electron wind force. The electrons collided with Cu atoms when a current was applied to the Sn/Cu/Sn interconnect. As a result, Cu atoms flowed from the cathode side to the anode side and led to the formation of the thicker IMCs at the anode side. Under the high current at the high temperature, vacancies were driven to flow to the cathode side. Once vacancies were supersaturated, cracks may be formed at the cathode side. Fig. 7(a) shows a microcrack formed at the cathode side (at the interface between the interfacial IMCs and Sn) after being applied with the current density of 1.0×10^4 A/cm^2 at 150 °C for 100 h, and the interconnect almost failed after EM for 200 h. However, there were no cracks observed at the anode side; and there were also no cracks observed at the cathode side at 150 °C under lower current density of 5.0×10^3 A/cm^2 and at lower temperature of 100 °C. Gan and Tu [12] also found the cracks formed at the cathode side when the Cu/Sn–3.8Ag–0.7Cu/Cu interconnect was applied with a current density of 3.2×10^4 A/cm^2 at 180 °C for 21 h. It is considered that the directional electron flow would deliver its momentum to the atoms. Therefore, the atoms moved from the cathode side toward the anode side and then a back stress generated which would result in voids at the cathode side. More voids would accumulate and thus microcracks would generate as EM time increasing. If a microcrack formed in a real flip chip solder joint, they will deteriorate the reliability of the solder joint.

The total thicknesses of the interfacial IMCs of Cu_6Sn_5 and Cu_3Sn as a function of the square root of time were plotted in Figs. 8 and 9. There was a linear relationship between the thickness of the IMCs and the square root of the aging time, indicating the growth kinetics of the interfacial IMCs followed the $t^{1/2}$ law during aging and the interfacial reaction during aging was dominated by the diffusion process. Similarly, the growth kinetics of the IMCs at the anode side also followed the $t^{1/2}$ law. However, the growth kinetics of the interfacial IMCs at the anode side during EM was significantly higher than that of the aging case. Table 1 summarizes the growth rate constant K, which represents the slope of the plot, under different conditions. Evidently, EM significantly enhanced the growth

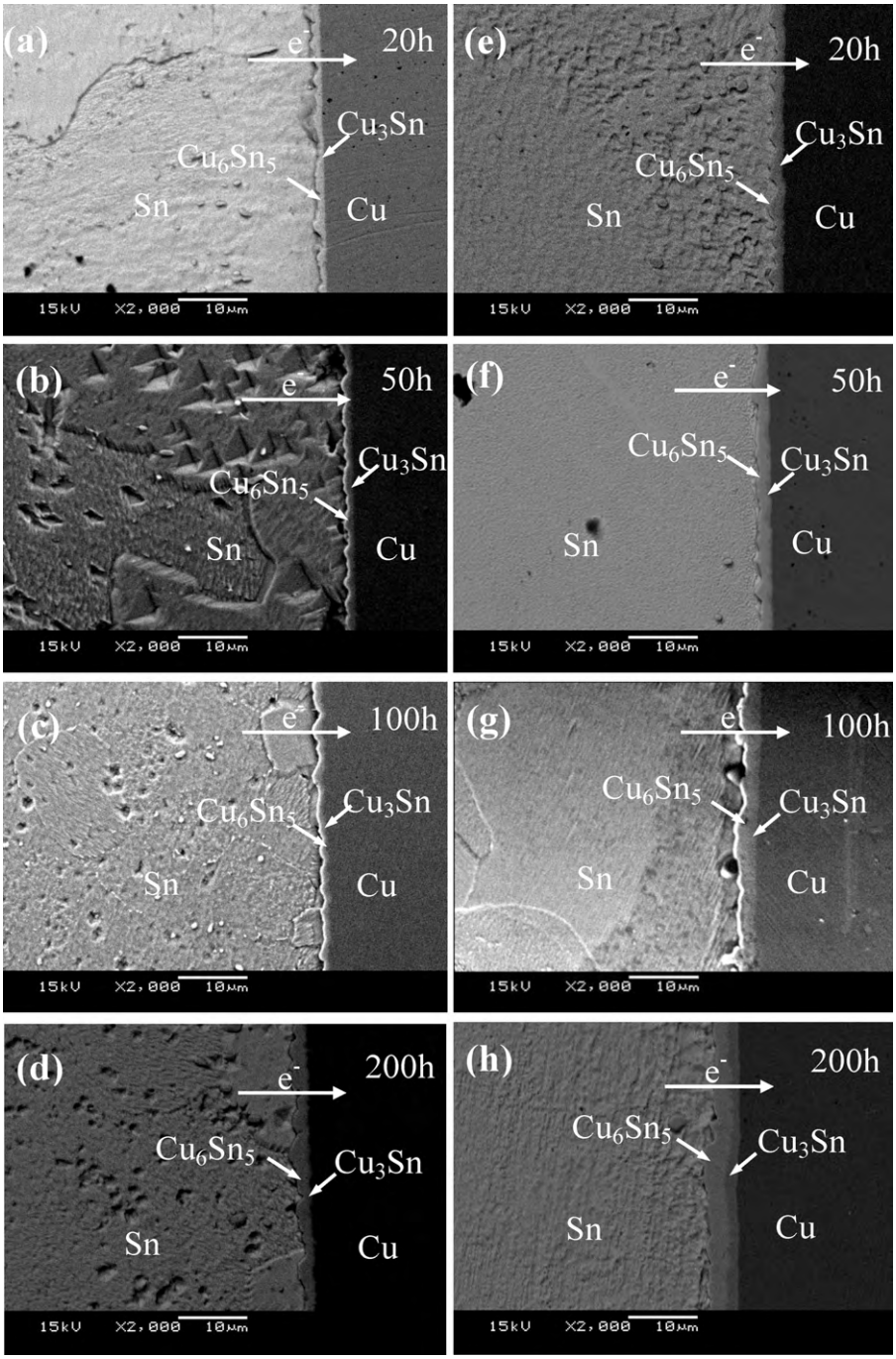

Fig. 5. SEM micrographs of the Sn/Cu interfaces (at the anode side) applied with current at 100 °C for various times: (a–d) with a current density of 5.0×10^3 A/cm^2 and (e–h) with a current density of 1.0×10^4 A/cm^2.

kinetics of the interfacial IMCs at the anode side compared with that of the aging case. Furthermore, the higher the temperature was, the faster the IMCs grew under the same current density during EM. This indicated that the temperature was one of the critical factors that influenced the EM.

The growth behavior of the interfacial IMCs at the cathode side was different from that at the anode side, as shown in Figs. 8 and 9. When the interconnects were applied with the current densities of 5.0×10^3 and 1.0×10^4 A/cm^2 at 100 °C, the IMCs at the cathode side increased at first 50–100 h and then decreased. When the interconnects were applied with the current density of 5.0×10^3 A/cm^2 at 150 °C, the IMCs at the cathode side continuously increased with the increasing EM time up to 200 h, while the IMCs at cathode side increased at first 50 h and then decreased under the current density of 1.0×10^4 A/cm^2 at 150 °C.

The growth behavior of the IMCs at the cathode side was complicated. When different current densities were applied at the different temperatures, the growth behavior of the interfacial IMCs was also different. The literature on the growth of the IMCs at the cathode side was limited and confused. Liu et al. [13] also found that the IMCs at the cathode side kept growing when the interconnect was applied with a current density of 5.3×10^3 A/cm^2 at 155 °C. Chan and co-workers [14] used Cu/SnBi/Cu interconnect to study the EM effect on the IMCs growth and found that the growth of the IMC layers both at the anode side and at the cathode side was enhanced when the interconnects were applied with a current

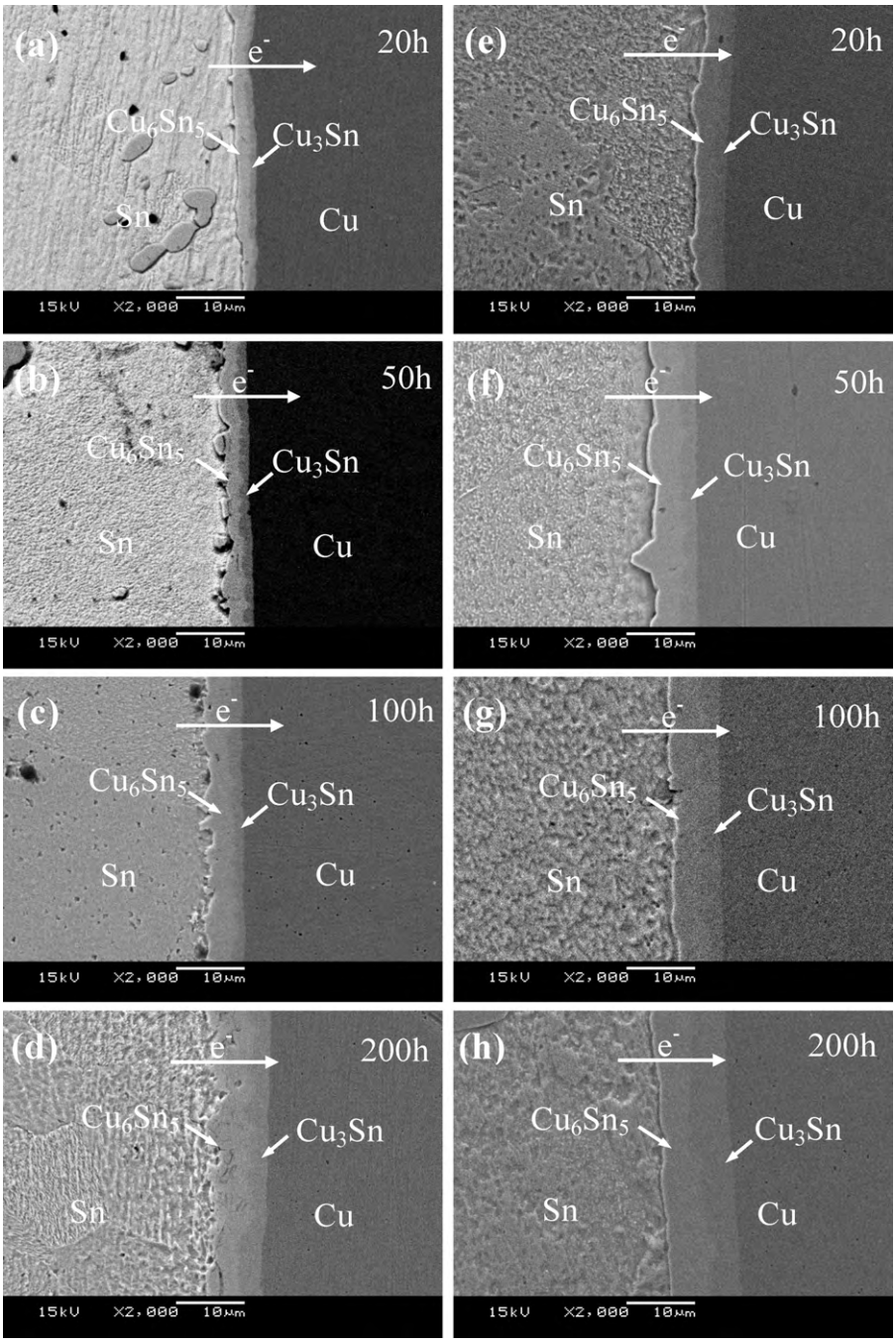

Fig. 6. SEM micrographs of the Sn/Cu interfaces (at the anode side) applied with current at 150 °C for various times: (a–d) with a current density of 5.0×10^3 A/cm^2 and (e–h) with a current density of 1.0×10^4 A/cm^2.

density of 5.0×10^3 A/cm^2 at 35 °C, 55 °C and 75 °C. Kao and co-workers [15] found the IMCs at the cathode side increased when the Cu/Sn-3.5Ag/Cu interconnect was applied with the current density of 6.3×10^3 A/cm^2 at 200 °C. In the present work, the IMCs at the cathode side continuously increased up to 200 h under the current density of 5.0×10^3 A/cm^2 at 150 °C, which was attributed to the thin initial IMCs thickness (less than 0.5 μm). Similarly, the initial IMCs thickness in the study by Chan and co-workers [14] was also less than 0.5 μm.

On the other hand, Ou and Tu [16] found that the growth of the IMCs at the cathode side (the specimen was aged at 150 °C for 200 h before EM) decreased first and then exhibited different growth behavior when different current densities were applied. The decrease in the IMCs thickness at the cathode side was attributed to high dissolution rates of the IMCs at the cathode side into solder matrix. The current may enhance the diffusion of Cu in the IMCs since Cu is the dominant diffusing species in the IMC growth [17].

It is concluded that the growth behavior was influenced by three factors: the initial IMC thickness, the current density and the temperature. To illustrate the effect of EM on the IMC formation, a growth model of the interfacial IMC at the cathode side was established. Fig. 10 shows the schematic of Cu flux at the cathode side. J_{em} is the drift term of Cu in the IMCs due to electron momentum transfer effect, J_{chem} is the diffusion term due to chemical potential gradient, and J_{dis} is the diffusion term due to the IMCs dissolution into the Sn. J'_{em} is the diffusion term of Cu in Sn due to electron momentum transfer effect. The diffusion coefficient of Cu in Sn was

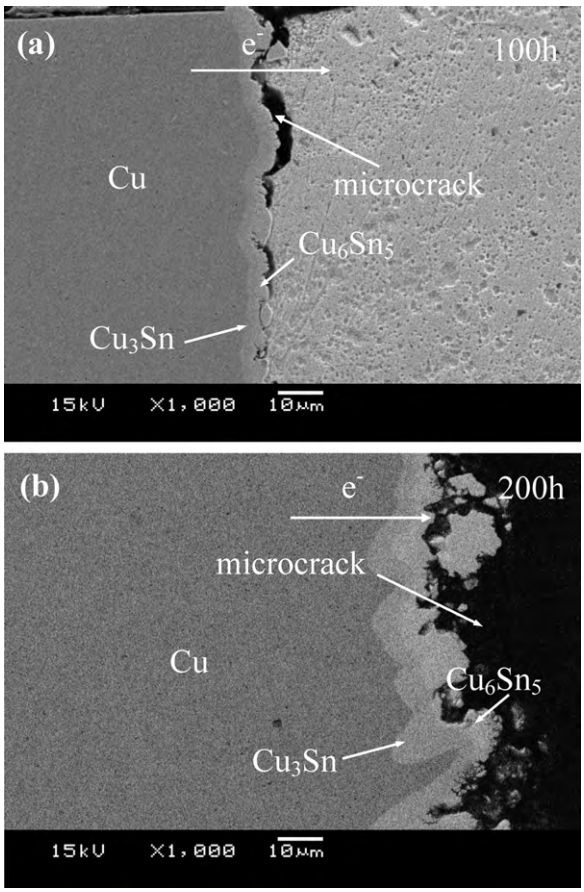

Fig. 7. Microcracks occurred at the cathode side after being applied with current density of 1.0×10^4 A/cm^2 at 150 °C for (a) 100 h and (b) 200 h.

reported to be 2.5×10^{-7} cm^2/s at 160 °C [18]. It is implied that once Cu atoms have dissolved into Sn, they would be instantaneously transported away from the cathode interface. The Cu concentration in the bulk of Sn near the IMC/Sn interface became unsaturated and Cu atoms in the IMCs continued to dissolve into the bulk of Sn. So J_{dis} plays an important rule at cathode side:

$$J = J_{em} + J_{chem} - J_{dis} = -D\left(\frac{\partial C}{\partial x}\right) + \left(\frac{CD}{kT}\right)\rho j Z^* e - J_{dis} \quad (3)$$

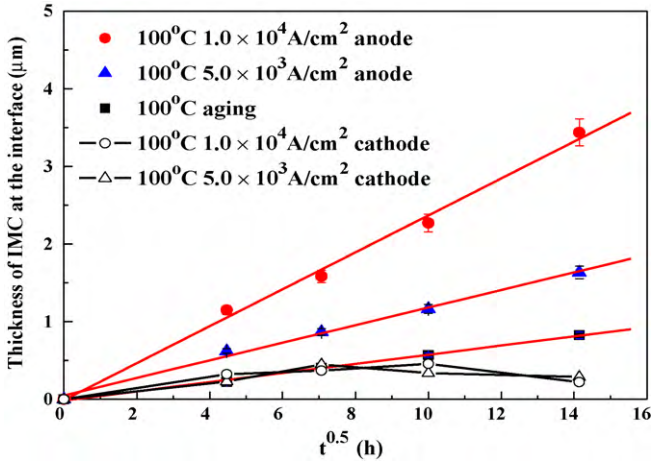

Fig. 8. The interfacial IMC thicknesses as a function of the square root of time at 100 °C.

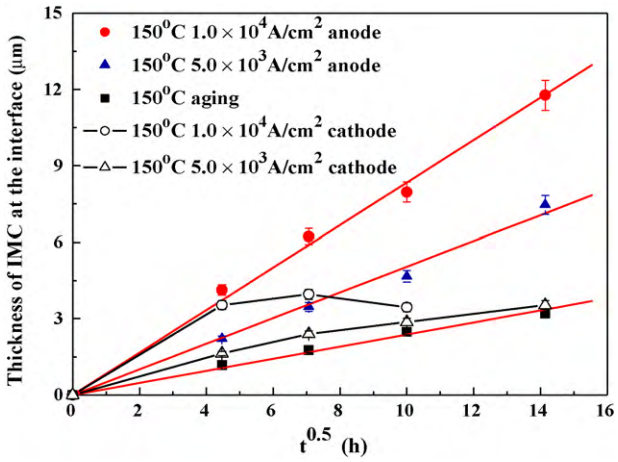

Fig. 9. The interfacial IMC thicknesses as a function of the square root of time at 150 °C.

Table 1
K values at the anode side under different conditions (cm s$^{-1/2}$).

Temperature	Aging	EM 5.0×10^3 A/cm^2	EM 1.0×10^4 A/cm^2
100 °C	9.83×10^{-8}	1.89×10^{-7}	3.96×10^{-7}
150 °C	3.81×10^{-7}	9.20×10^{-7}	1.40×10^{-6}

where C is the concentration, D is the diffusivity, k is Boltzmann's constant, T is the absolute temperature, ρ is the resistivity, and j is the current density, Z^* is the effective charge number, and e is the electron charge.

From Eq. (3), the thickness of the IMCs at the cathode side was determined by J_{em}, J_{chem}, and J_{dis}. At the initial stage the interfacial IMCs was very thin at the cathode side. The chemical potential was large, while J_{dis} was minute compared with $J_{em} + J_{chem}$, thus the J_{dis} effect can be ignored. The inward atomic fluxes were larger than the outward fluxes, and thus the thickness of the IMCs increased at first. When the interfacial IMCs at the cathode side became thick enough, the chemical potential, i.e., the diving force for Cu atoms to diffuse to the interface, would decrease. The J_{dis} term became lager than $J_{em} + J_{chem}$. The inward atomic fluxes were less than the outward fluxes, and thus the thickness of the IMCs decreased. When the IMCs was very thin, the interfacial IMCs increased at first, and the interfacial IMCs decreased after a critical thickness was reached.

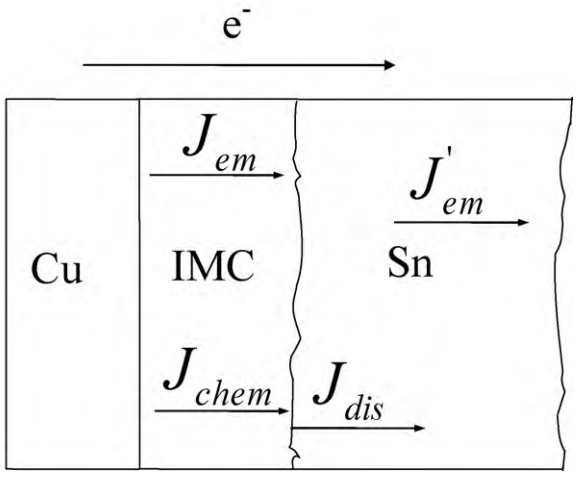

Fig. 10. Schematic diagram of Cu flux at the cathode side in the EM specimen.

4. Conclusions

The growth kinetics of interfacial IMCs in the line-type Cu/Sn/Cu interconnects during EM and aging was investigated. EM caused a polarity effect, i.e., the interfacial IMCs at the anode side were thicker than those at the cathode side. The initial scallop-type interfacial Cu_6Sn_5 IMC in as-soldered state gradually transformed into layer-type IMC during both EM and aging. The growth kinetics of the interfacial IMCs at the anode side during EM was significantly enhanced compared with that of the aging (no-current case), and still followed the $t^{1/2}$ law with time. The interfacial IMCs at the anode side grew faster under higher current density at the same temperature. The temperature was one of the critical factors that influenced the EM. The effect of EM became more significant at higher temperature under the same current density. The growth rate constant of the IMCs at the anode side was 1.40×10^{-6} cm s$^{-1/2}$ under the current density of 1.0×10^4 A/cm^2 at 150 °C compared with that of 3.81×10^{-7} cm s$^{-1/2}$ during aging at 150 °C; and 3.96×10^{-7} cm s$^{-1/2}$ under the current density of 1.0×10^4 A/cm^2 at 100 °C compared with that of 9.83×10^{-8} cm s$^{-1/2}$ during aging at 100 °C.

The growth behavior of the interfacial IMCs at the cathode side was different from that at the anode side. The dissolution of the IMCs at the cathode side played an important role. Due to the thin initial interfacial IMCs (less than 0.5 μm) in the as-soldered state, the inward atomic fluxes were larger than the outward fluxes, and thus the IMCs increased at the first stage of EM. After the IMCs at the cathode side increased to a critical thickness, the J_{dis} term became lager than the $J_{em} + J_{chem}$ term, i.e., the inward atomic fluxes were less than the outward fluxes, and thus the thickness of the IMCs decreased. After being applied with a current density of 1.0×10^4 A/cm^2 at 150 °C for 100 h, mircocracks formed at the cathode side between the solder and the interfacial IMCs, while in this study there were no cracks observed when the interconnects were applied with a current density of 5.0×10^3 A/cm^2 at 150 °C, and also no cracks were observed when the interconnects were applied with current densities of 5.0×10^3 and 1.0×10^4 A/cm^2 at 100 °C.

Acknowledgments

This work is supported by the programs of National Natural Science Foundation of China (Nos. U0734006 and 50811140338), the programs in Liaoning Province (Nos. 20060133, 2009921058 and 20082163), and the Research Fund for the Doctoral Program of Higher Education in China (No. 20070141062).

References

[1] K.N. Tu, A.M. Gusak, M. Li, J. Appl. Phys. 93 (2003) 1335–1353.
[2] E.C.C. Yeh, W.J. Choi, K.N. Tu, Appl. Phys. Lett. 80 (2002) 580–582.
[3] D. Yang, B.Y. Wu, Y.C. Chan, K.N. Tu, J. Appl. Phys. 102 (2007) 043502.
[4] A. Kumar, Y. Yang, C.C. Wong, Z. Chen, J. Electron. Mater. 38 (2009) 78–87.
[5] W.H. Wu, H.L. Chung, C.N. Chen, C.E. Ho, J. Electron. Mater. 38 (2009) 2563–2572.
[6] C.M. Chen, C.C. Huang, J. Alloys Compd. 461 (2008) 235–241.
[7] H.J. Lin, J.S. Lin, T.H. Chuang, J. Alloys Compd. 487 (2009) 458–465.
[8] X.F. Zhang, J.D. Guo, J.K. Shang, J. Mater. Res. 23 (2008) 3370–3378.
[9] K. Yamanaka, Y. Tsukada, K. Suganuma, J. Alloys Compd. 437 (2007) 186–190.
[10] B.Y. Wu, Y.C. Chan, J. Alloys Compd. 392 (2005) 237–246.
[11] C.M. Chen, Y.M. Huang, C.H. Lin, J. Alloys Compd. 475 (2009) 238–244.
[12] H. Gan, K.N. Tu, J. Appl. Phys. 97 (2005) 063514.
[13] C.Y. Liu, L. Ke, Y.C. Chuang, S.J. Wang, J. Appl. Phys. 100 (2006) 083702.
[14] X. Gu, D. Yang, Y.C. Chan, B.Y. Wu, J. Mater. Res. 23 (2008) 2591–2596.
[15] J.R. Huang, C.M. Tsai, Y.W. Lin, C.R. Kao, J. Mater. Res. 23 (2008) 250–257.
[16] S.Q. Ou, K.N. Tu, Proceedings of the 55th Electronic Components and Technology Conference, 2005, pp. 1445–1450.
[17] K.N. Tu, R.D. Thompson, Acta Mater. 30 (1982) 947–952.
[18] B.F. Dyson, T.R. Anthony, D. Turnbull, J. Appl. Phys. 38 (1967) 3408–3409.